NEUROSCIENCE

Hyperexcited limbic neurons represent sexual satiety and reduce mating motivation

Xiaojuan Zhou[1]†, Ang Li[1,2]†, Xue Mi[1]†, Yixuan Li[1,2], Zhaoyi Ding[1], Min An[1], Yalan Chen[1], Wei Li[1], Xianming Tao[1], Xinfeng Chen[1,2], Ying Li[1]*

Transient sexual experiences can have long-lasting effects on behavioral decisions, but the neural coding that accounts for this change is unclear. We found that the ejaculation experience selectively activated estrogen receptor 2 (*Esr2*)–expressing neurons in the bed nucleus of the stria terminalis (BNST)—BNST^{Esr2}—and led to persistent decreases in firing threshold for days, during which time the mice displayed sexual satiety. Inhibition of hyperexcited BNST^{Esr2} elicited fast mating recovery in satiated mice of both sexes. In males, such hyperexcitability reduced mating motivation and was partially mediated by larger HCN (hyperpolarization-activated cyclic nucleotide-gated) currents. Thus, BNST^{Esr2} not only encode a specific mating action but also represent a persistent state of sexual satiety, and alterations in a neuronal ion channel contribute to sexual experience–dependent long-term changes to mating drive.

Transient social experiences (such as a sexual experience) can lead to long-lasting changes in internal states and affect social behaviors, such as mating, aggression, and parental care (*1*–*3*). For example, after successful mating with ejaculation, many species quickly display an inhibition of the tendency to mate for hours, days, or longer, an effect known as sexual satiety (*4*). This inhibition is essential not only for avoiding excessive risk-taking or the energy-consuming search for new sexual partners but also for increasing the fertilization rate (*5*). Yet relatively little is known about how such experience-dependent changes are represented in neural circuits and result in long-lasting effects on behavioral decisions.

Experiencing ejaculation drives sexual satiety in both sexes

When we presented a male mouse with a female mouse in estrus, the male typically began to investigate the female and attempted to mount her within minutes, during which time the female played an active role by either showing receptive behavior (lordosis) or rejecting the male (by sitting down or fleeing) (Fig. 1A and movie S1). After mating successfully, males and females typically lose interest in sexual behavior (*6*, *7*), with substantial effects on both the readiness to transition from copulatory-seeking behavior to mating and the execution of different mating actions, which gradually returns over several days to weeks (Fig. 1, B to D, and fig. S1). In female mice, experiencing ejaculation by vasectomized male mice (referred to as the ejaculatory reflex) can suppress sexual receptiveness soon after mating (Fig. 1, C and D) and induce luteal activity for ~2 weeks (fig. S1, E to H) (*7*). However, no such change was observed in mice that experienced multiple intromissions but were separated from their partner before ejaculation (Fig. 1, B to D).

Ejaculation selectively activates *Esr2*-expressing BNSTpr neurons

In rats and gerbils, ejaculation-induced expression of c-Fos is present in different brain regions corresponding to successive stages of the vomeronasal pathway, including the posterior bed nucleus of the stria terminalis (BNSTp), posterodorsal medial amygdala (MeApd), and medial subparafascicular thalamic nucleus (mSPF), but not the median preoptic nucleus (MPN) (*8*, *9*). These have been identified to play key roles in transforming neural representation of external social cues into behavioral decisions that drive sex-specific mating actions (*10*–*19*). Using fluorescence in situ hybridization (FISH), we examined which brain regions were preferentially active in ejaculated male mice as compared with those that experienced multiple intromissions without ejaculation (fig. S2A). We observed the highest fold-change in the number of *Fos*$^+$ neurons in the BNSTp and, to a lesser extent, in the MeApd, but there were no significant changes in the mSPF or MPN (fig. S2, B and C). At the anatomical level, BNSTp neurons send major projections to the MeA and hypothalamic areas (*20*), both of which show stable changes in representing conspecific social cues after a sexual experience (*21*, *22*). Therefore, we sought to examine the genetic identity of the ejaculation-activated neurons in the BNSTp and whether they encode sexual experience–dependent changes and regulate behavioral decisions in the long term.

According to recent single-nuclei RNA sequencing (snRNA-seq), the principal nucleus of the BNST (BNSTpr) contains two sexually dimorphic neuronal clusters that express either estrogen receptor 2 (*Esr2*) or suppression of tumorigenicity 18 (*St18*) (*23*). Using multiplex FISH, we determined that BNSTpr neurons expressing *Esr2* (BNST^{Esr2}) located in both the dorsal and ventral compartments were activated after ejaculation, whereas *St18*-expressing neurons (BNST^{St18}) were preferentially activated during male-female interactions before ejaculation (fig. S3). To directly monitor BNST^{Esr2} or BNST^{St18} activity during mating, we performed single cell–resolution Ca^{2+} imaging using head-mounted microendoscopes in freely behaving *Esr2-Cre* or *St18-Cre* mice (Fig. 1E and fig. S5A; evaluation of both mouse lines is provided in fig. S4). In both sexes, a majority of BNST^{Esr2} were activated by social sniffing and ejaculation but not by other mating actions (Fig. 1G and fig. S5B). This response contrasts with that in BNST^{St18}, most of which were activated by social sniffing and intromission but not by ejaculation (Fig. 1I and fig. S5E). Moreover, distinct BNSTpr neuronal subsets that were activated by either ejaculation or other mating actions, although spatially intermingled (fig. S5, C and F), were for the most part distinct from neurons activated during early social sniffing, with the relative activity of each neuron during sexual behaviors and during sniffing being negatively correlated (fig. S5, D and G).

Ejaculation-induced BNST^{Esr2} activation dramatically decreased in both sexes after males and females were separated, but the postejaculatory spontaneous activity in individual neurons differed. As compared with the baseline before an intruder was introduced, some BNST^{Esr2} were transiently activated during ejaculation, whereas others displayed higher spontaneous activities for 1 to 2 min after ejaculation (fig. S6, A to C). Such persistent activation typically lasted throughout the rest of the recording period (5 to 30 min) during a single day and was gradually reduced over time, although the time constant after which this activation was no longer significantly different from the baseline was unclear (Fig. 1F and fig. S6, D and E). These results suggested that a subset of ejaculation-activated BNST^{Esr2} may encode persistent changes in internal states after successful mating. By contrast, nearby nonoverlapping BNST^{St18} consisted of neurons that were selectively activated during sniffing an opposite-sex intruder (fig. S5, E to G) or during mating actions other than ejaculation (Fig. 1H).

Hyperactivated BNST^{Esr2} encode sexual satiety

Male BNSTpr neurons that express *Aromatase* (BNST^{Arom}) respond differently to the two sexes (*17*). Using FISH, we found that 37% of

[1]Chinese Institute for Brain Research, Beijing 102206, China. [2]Academy for Advanced Interdisciplinary Studies, Peking University, Beijing 102206, China.
*Corresponding author. Email: liying@cibr.ac.cn
†These authors contributed equally to this work.

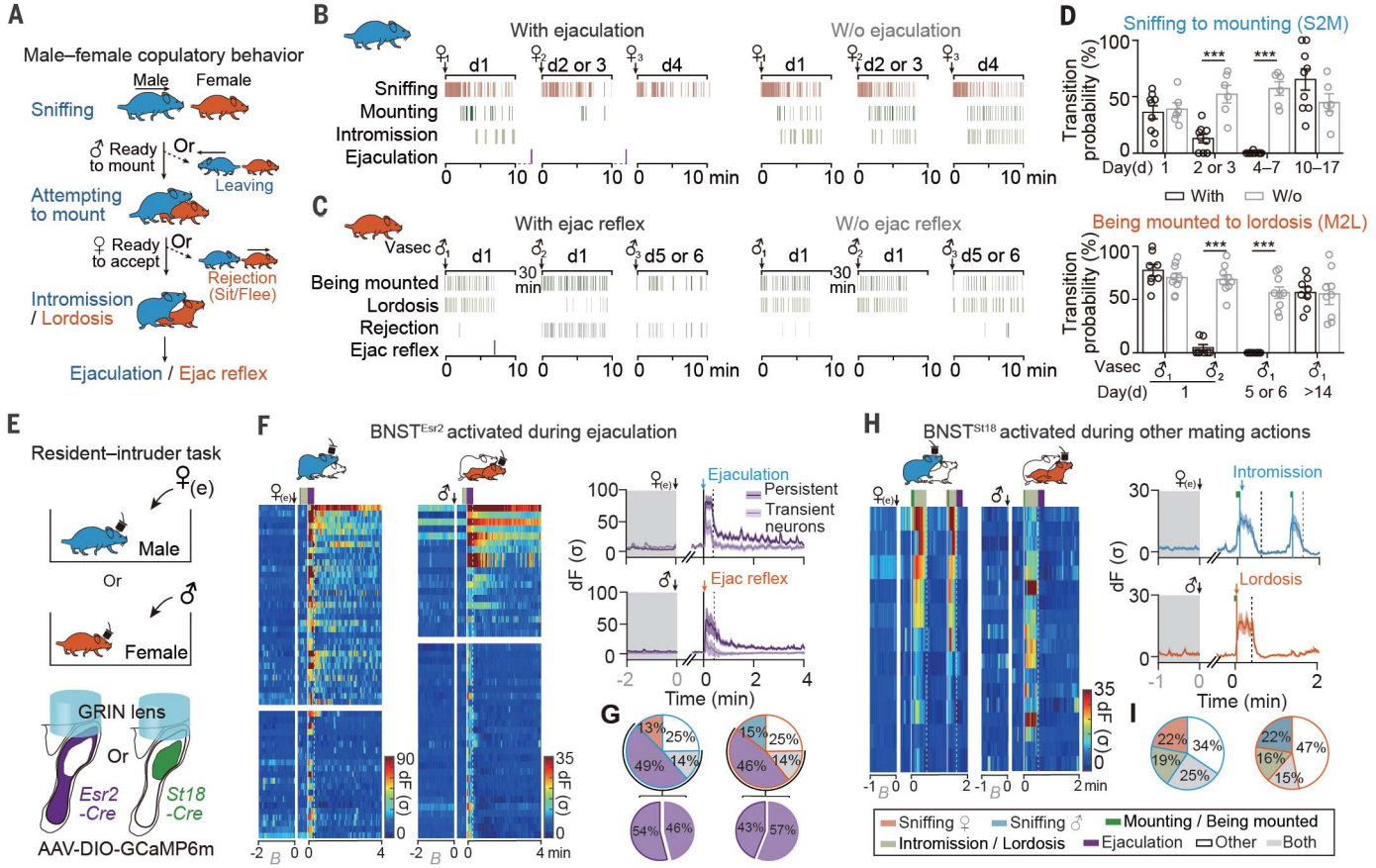

Fig. 1. Ejaculation drives sexual satiety and selectively activates *Esr2* neurons in the BNSTpr of both sexes. (**A**) Typical male and female mating behaviors in mice. (**B** and **C**) Behavioral events of (B) male or (C) female virgin mice 10 min after the initial sniffing of female intruders on consecutive days or being mounted by two different vasectomized (vasec) male mice on day 1 (d1) and by a new male on d5 or d6 (theoretically in another estrous cycle). Males either (left) were allowed to ejaculate during mating or (right) were separated from the female before ejaculation. (**D**) The probability of transitioning from copulatory-seeking behavior to mating in (top) male and (bottom) female mice during the period shown in (B) and (C). Data are shown as the mean ± SEM. Mann-Whitney *U*-test was used; ***$P < 0.001$. (**E**) (Top) Experimental design and (bottom) schematic of microendoscopic Ca^{2+} imaging. e, in estrus; GRIN, gradient index. (**F** and **H**) Heatmaps of representative Ca^{2+} activity of (F) $BNST^{Esr2}$ or (H) $BNST^{St18}$ before intruder introduction (spontaneous baseline, *B*) and corresponding to the experience of (F) ejaculation or (H) other mating actions in (left) males and (right) females. Colored bars at the top indicate mating behaviors as defined in (H). Line charts show averaged Ca^{2+} activity of neurons in each subpopulation; shading indicates SEM. Solid and dashed vertical lines indicate onset and offset of different mating actions, respectively. (**G** and **I**) Fractions of (G) $BNST^{Esr2}$ or (I) $BNST^{St18}$ activated during different behavioral events. Bottom pie charts in (G) show fractions of ejaculation-responsive neurons displaying either persistent or transient activation. In (G), data are from 323 neurons from four males and 197 neurons from four females. In (I), data are from 64 neurons from two males and 184 neurons from three females.

$BNST^{Arom}$ express *Esr2*, whereas 35% express *St18* (fig. S7). The activities of male $BNST^{Esr2}$ and $BNST^{St18}$ were greater upon introduction of a female intruder as compared with a male intruder (fig. S8, A and B). However, such responses subsided significantly in $BNST^{Esr2}$, but not in $BNST^{St18}$, during later investigations (fig. S8C), particularly after the first mount (fig. S8D).

To further examine whether $BNST^{Esr2}$ activity encoded sexual satiety, socially isolated (for at least 1 day) male mice were allowed to interact with a female intruder in either estrus or diestrus and then were tested again with a different estrous female 24 hours later (Fig. 2A). Four out of five of the examined male mice were able to perform another mating 24 hours after ejaculation (Fig. 2B), suggesting that they were not fully satiated before mating on day 2. As compared with the baseline activity on day 1, only behaviorally satiated mice displayed spontaneous Ca^{2+} transients that had larger amplitudes and occurred more frequently (Fig. 2C, group 3). Such an increase could last throughout the sexual refractory period for days and returned to the baseline level associated with virgin mice once the mice were ready to mate again; the increase quickly occurred again after another ejaculation-induced sexual satiety (fig. S9, A to C). By contrast, in the unmated (group 1) or recently mated but unsatiated (group 2) males, spontaneous Ca^{2+} transients of $BNST^{Esr2}$ remained stable 24 hours after the social experience (Fig. 2C). As another indicator of encoding sexual satiety in $BNST^{Esr2}$, the spontaneous Ca^{2+} transients (Fig. 2D) and the activity of $BNST^{Esr2}$ upon the introduction of a female intruder (fig. S8E) negatively correlated with the readiness to transition from sniffing to mounting.

Similarly, in sexually satiated females, the amplitude and frequency of spontaneous Ca^{2+} transients were also increased regardless of fertilization state (Fig. 2, E and F). Such increases typically lasted throughout pseudopregnancy or pregnancy and the period of lactation and decreased to baseline levels associated with virgin females after behavioral recovery (fig. S9, D to F). However, the spontaneous Ca^{2+} transients in $BNST^{Esr2}$ from virgin females in estrus versus diestrus were similar

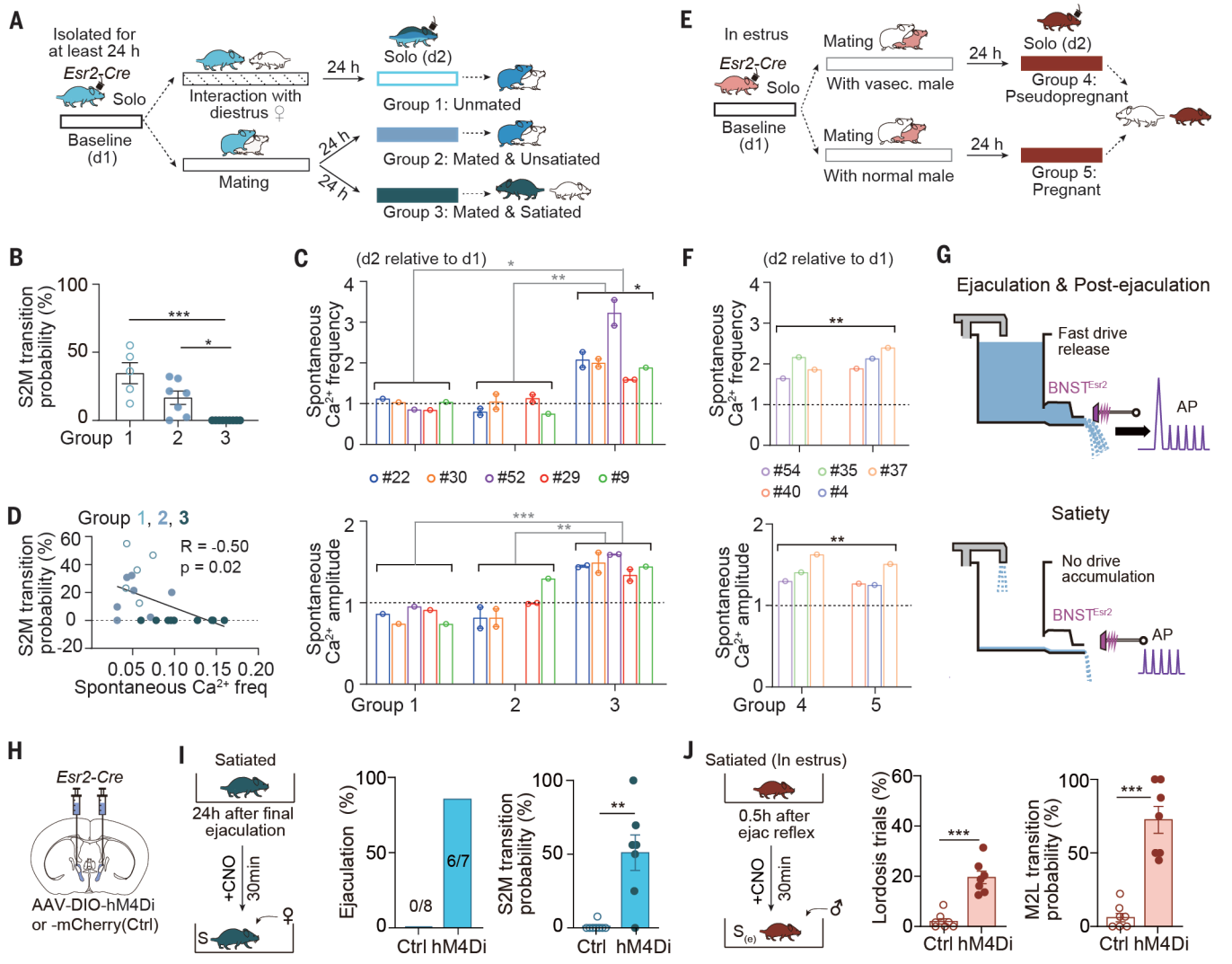

Fig. 2. Hyperactivated BNST^{Esr2} encode persistent sexual satiety in both sexes. (**A** and **E**) Examining the spontaneous Ca^{2+} activity of BNST^{Esr2} in individually isolated (A) male and (E) female mice before day 1 (d1) and 24 hours after d2 exposure to an opposite-sex intruder. (**B**) Probability of transitioning from sniffing to mounting (S2M; 10 min after initial sniffing) in unmated (group 1; five trials from five mice), mated and unsatiated (group 2; seven trials from four mice), and mated and satiated (group 3; nine trials from five mice) males on day 2. (**C** and **F**) Averaged (top) frequency and (bottom) amplitude of spontaneous Ca^{2+} transients of BNST^{Esr2} in (C) male and (F) female mice on day 2. The data point from each mouse was normalized to its baseline value on day 1. Comparison was done for each group with the baseline unless otherwise specified. The #37 female was first exposed to a vasectomized male and then was exposed to an intact male after behavioral recovery. (**D**) Correlation between the probability of transitioning from sniffing to mounting and the averaged spontaneous Ca^{2+} frequency of BNST^{Esr2} in each mouse. (**G**) A hydraulic model to reconcile the responses of BNST^{Esr2} during ejaculation, soon after ejaculation, and during sexual satiety. (**H**) Strategy to bilaterally express hM4Di or mCherry (control) in BNST^{Esr2}. (**I** and **J**) Behaviors of sexually satiated (I) male and (J) female mice exposed to an opposite-sex intruder, 30 min after CNO injection. M2L, transitioning from being mounted to lordosis. In (B) and (C), Kruskal-Wallis test with Dunn's multiple comparisons correction was used. In (F), (I), and (J), Mann-Whitney *U*-test was used; $^*P < 0.05$, $^{**}P < 0.01$, $^{***}P < 0.001$. For all relevant panels, data are shown as the mean ± SEM.

but were lower than those in virgin males (fig. S9, G to I).

To investigate whether persistent activation of BNST^{Esr2} is necessary to maintain sexual satiety, we expressed G_i-coupled DREADD (designer receptor exclusively activated by designer drugs) hM4Di bilaterally in the BNST of *Esr2-Cre* mice (Fig. 2H). In six of seven satiated males, inhibition of BNST^{Esr2} by means of intraperitoneal injection of clozapine-*N*-oxide (CNO) restored their mating behavior in 30 min and led to ejaculation (Fig. 2I), with the readiness to transition from sniffing to mounting comparable with that in virgin males (fig. S10, A to C). The same manipulation largely restored sexual receptiveness in recently mated females (Fig. 2J and fig. S10, D and E), who typically show a reduced interest in males (*24*). Similar deficits in achieving sexual satiety were also observed in BNST^{Esr2}-ablated mice of both sexes after consecutive ejaculation experiences (fig. S11).

Activation of male BNST^{Esr2} reduces mating motivation

In virgin males, both chemogenetic silencing and ablation of BNST^{Esr2} induced more frequent mounting behaviors toward male intruders, whereas chemogenetic silencing additionally increased their readiness to transition from sniffing to mounting toward female intruders and delayed the ejaculation latency by almost twofold (figs. S11D and S12, A to C). However, chemogenetic inhibition of BNST^{Esr2}

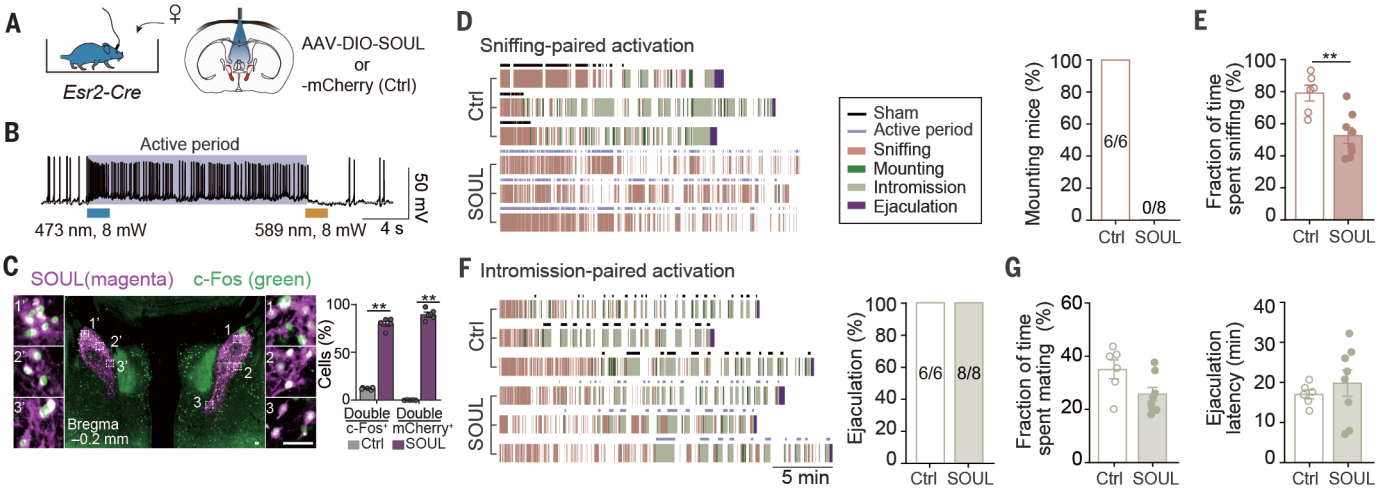

Fig. 3. Optogenetic activation of BNST^{Esr2} during early sniffing selectively inhibits male intention to mate. (**A**) Transcranial optical stimulation through the intact skull of virgin male mice. (**B**) Current-clamp traces illustrating activation of a SOUL-expressing BNST^{Esr2} in acute brain slices upon blue-light activation (blue bar) and orange-light deactivation (orange bar). (**C**) Colabeling of SOUL (magenta) and c-Fos (green) in a coronal BNST section, with boxed regions magnified after photostimulation. Scale bar, 50 μm. (Right) Overlap between mCherry and c-Fos expression. (**D** to **G**) Behaviors of males associated with [(D) and (E)] sniffing-paired or [(F) and (G)] intromission-paired photostimulation of BNST^{Esr2}. Shown in (D) and (F) (left) are behavior raster plots and the active period as in (B), and (right) are fraction of males that either (D) initiated mounting within 15 min or (F) ejaculated. Mann-Whitney *U*-test was used; $^{**}P < 0.01$, $^{***}P < 0.001$. For (A) to (G), data are shown as the mean ± SEM.

in virgin females did not overcome the effect of cycling hormones that increased their sexual receptiveness (fig. S12, D and E). Because female BNST^{Esr2} displayed less frequent firing rates than that of male ones during baseline before an intruder was introduced (fig. S9I), further inactivation may be less effective in up-regulating mating performance in female mice.

Consistently, chemogenetic activation of BNST^{Esr2} strongly suppressed sexual behavior in male mice (fig. S13, A to C), which is contrary to the effect of activating BNST^{Arom} (*13*), *Esr1*-expressing neurons in the BNSTpr (BNST^{Esr1}) (*18*), or nearby nonoverlapping BNST^{St18} (fig. S13, E to G). However, such an effect was not observed in estrous female mice (fig. S13D). Chemogenetic activation of male BNST^{Esr2} could possibly suppress mounting actions and/or motivational states to carry out sexual behaviors. To distinguish between these possibilities, we expressed a step-function opsin with ultrahigh light sensitivity (SOUL) (*25*) and performed transcranial optical stimulation to noninvasively activate BNST^{Esr2} during different mating phases (Fig. 3A). Transient application of blue light resulted in persistent activation of SOUL-expressing neurons, which were largely suppressed by transient application of orange light, as verified with ex vivo recordings (Fig. 3B). Using this approach, we induced robust expression of c-Fos protein bilaterally in SOUL-expressing BNST^{Esr2} in behaving mice (Fig. 3C). Sniffing-paired activation of BNST^{Esr2} (occurred with the first sniffing of an intruder) was effective in suppressing the initiation of an attempted mount (Fig. 3D). This manipulation also reduced the fraction of time spent sniffing a female intruder during the premounting period in early investigation (within 10 min after the initial sniffing) (Fig. 3E), which largely mimicked the behaviors in sexually satiated male mice (fig. S1D). However, intromission-paired optogenetic activation (Fig. 3F) or inhibition (fig. S14) of BNST^{Esr2} (occurred with the first intromission) did not interrupt ongoing mating actions. These males spent a similar amount of time in mating (including both mounting and intromission) without affecting ejaculation latency from the first mount (Fig. 3G and fig. S14D).

Elevated expression of HCN in male BNST^{Esr2} mediates sexual satiety

To determine how transient mating experience may lead to persistent changes in BNST^{Esr2} activity that lasts for days, we recorded from fluorescently labeled BNST^{Esr2} with whole-cell patch clamp recording in brain slices from virgin, sexually satiated, and behaviorally recovered Esr2-Cre:histone 2b (H2B)–green fluorescent protein (GFP) mice of both sexes (fig. S15A). A higher fraction of BNST^{Esr2} exhibited spontaneous firing in satiated mice as compared with virgin or recovered mice and also displayed more frequent firing rates (fig. S15B). Despite comparable input resistance and membrane capacitance, the resting membrane potentials (RMPs) were highest and the rheobases (the most negative step current required to elicit all-or-none firing) were lowest in BNST^{Esr2} from satiated mice (fig. S15, C and D), which were thus primed to fire action potentials after smaller depolarization. Such changes were largely restored in behaviorally recovered mice.

The hyperexcitability of satiated BNST^{Esr2} suggested a change in ion channels that influences the firing pattern and spike threshold (*26*). Negative current injection in BNST^{Esr2} revealed a depolarizing voltage "sag," which is mainly mediated by hyperpolarization-activated cyclic nucleotide-gated (HCN) cation channels (Fig. 4A). In BNST^{Esr2} with substantial voltage sag (>10% of peak voltage), perfusion of a selective HCN blocker, ZD-7288 (20 μM), significantly reduced the size of the voltage sag and firing rates (Fig. 4B). In male (but not female) mice, the size of this voltage sag was larger in satiated versus virgin or recovered BNST^{Esr2} (Fig. 4C). However, such an increase was not observed in males at 30 min after ejaculation, during which time BNST^{Esr2} hyperexcitability was already presented (fig. S15E). Moreover, the fraction of BNST^{Esr2} that displayed substantial voltage sag in males was higher than that in females (Fig. 4D). To examine the functional relevance of HCN channels in regulating sexual satiety, we administered (intracranially) either ZD-7288 (1 mM) or artificial cerebrospinal fluid (ACSF; vehicle control) into both sides of the BNSTpr (250 nl each) of sexually satiated mice (fig. S16, A and B). Application of ZD-7288 significantly restored sexual behavior (including ejaculation) after

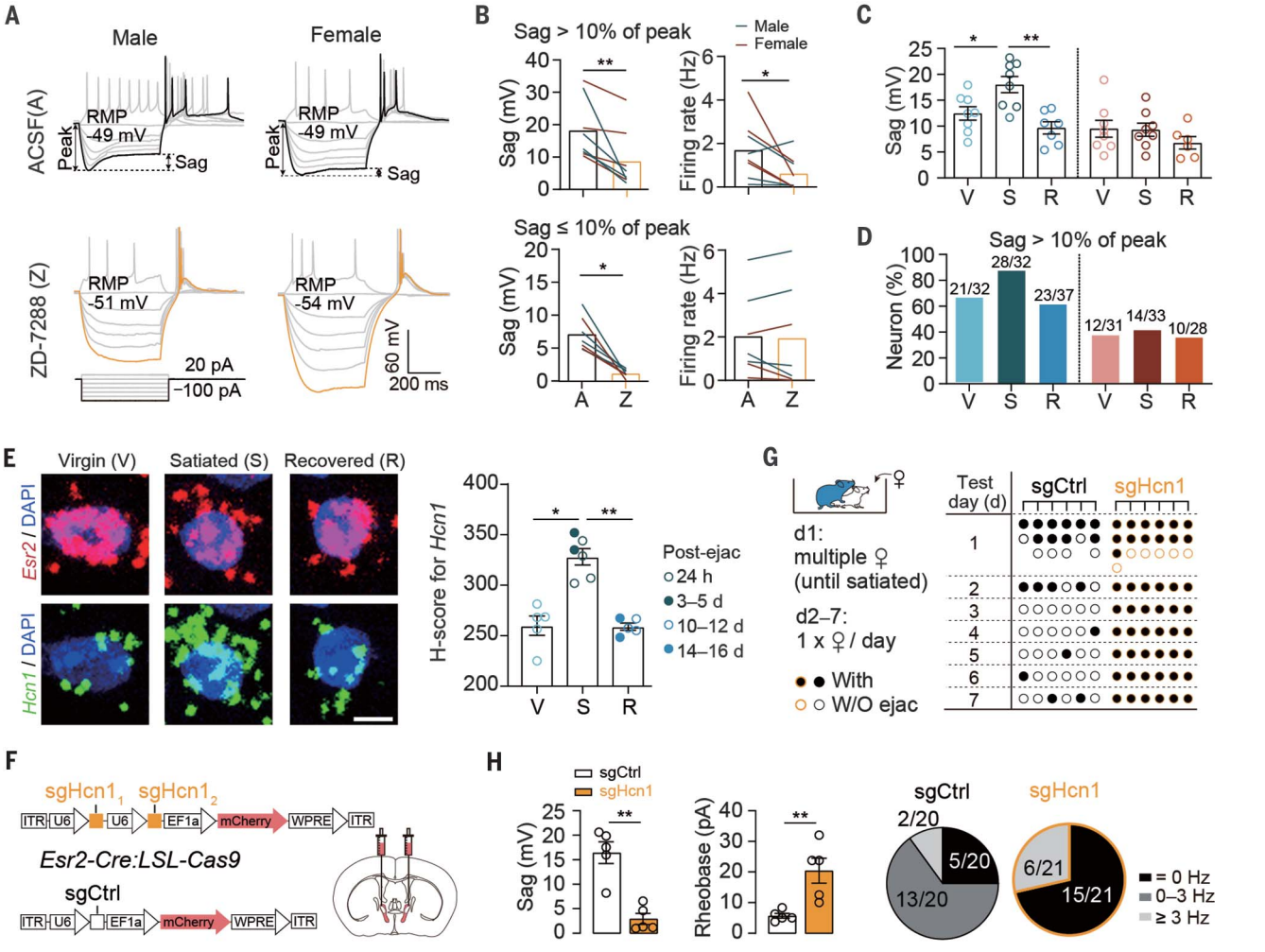

Fig. 4. Increased HCN currents (I_h) contribute to hyperexcitability of BNST^{Esr2} in sexually satiated male mice. (**A**) Current clamp recordings from BNST^{Esr2} in satiated (left) male or (right) female mice in response to 500-ms current steps (−100 to 20 pA, 20-pA step) (top) in the presence of ACSF or (bottom) 10 min after the perfusion of ZD-7288 (20 μM). The I_h-associated voltage sag was measured as the voltage deflection in response to a −100-pA step current. (**B**) The (left) size of voltage sag and (right) firing rates in BNST^{Esr2} (top) with or (bottom) without substantial voltage sag. Wilcoxon matched-pairs signed-rank test was used. (**C** and **D**) The (C) size of voltage sag in BNST^{Esr2} and (D) fraction of BNST^{Esr2} with substantial voltage sag in brain slices from virgin, satiated, and recovered (blue) male and (orange) female mice. In (C), one-way analysis of variance with Tukey's multiple comparisons test was used. In (D), the number of recorded neurons (three to six neurons per mouse) in each group is shown above each bar. (**E**) The expression of *Hcn1* mRNA in BNST^{Esr2} from virgin (12 sections from five mice), satiated (15 sections from six mice), or recovered males (10 sections from five mice). Scale bar, 5 μm. Kruskal-Wallis test with Dunn's multiple comparisons correction was used. (**F**) Schematic showing AAV sgControl and AAV sgHcn1 vector design and bilateral viral infection in the BNST. (**G**) Consecutive mating tests in males across 7 days at 2 to 3 weeks after virus injection (left). (**H**) Comparison of the (left) voltage sag and (middle) rheobase between sgControl (20 neurons from five satiated mice) and sgHcn1 (21 neurons from five mice with multiple ejaculations) group. Pie plots show fractions of neurons with different firing rates. Mann-Whitney *U*-test was used; $^*P < 0.05$, $^{**}P < 0.01$. For (B) to (D) and (H), data are shown as the mean ± SEM.

~1 hour in five of six satiated males but did not restore sexual receptiveness in recently mated females (fig. S16, C to G).

There are four mammalian subunits, referred to as HCN1 to HCN4, that constitute the molecular substrate of a persistent sodium current (also known as I_h) (*27*, *28*). On the basis of a systematic reanalysis of a published snRNA-seq dataset for the BNST (*23*), we found that *Hcn1*, but not the other subunits, was highly enriched in BNST^{Esr2} (fig. S17). To examine the levels of *Hcn1* before and at multiple times after ejaculation, we performed single-cell quantification of *Hcn1* mRNA in the BNSTpr using FISH. In male mice, the expression level of *Hcn1* [calculated as H-score (*29*)] in satiated BNST^{Esr2} was significantly higher than that in BNST^{Esr2} from virgin and recovered males (Fig. 4E). To further examine the self-autonomous function of *Hcn1* on BNST^{Esr2}, we crossed *Esr2-Cre* mice with mice in which Cre-dependent Cas9–enhanced GFP (EGFP) was inserted (*30*) and applied adeno-associated virus (AAV)–mediated expression of a single-guide RNA (sgRNA) (sgControl or sgHcn1) bilaterally to the BNST (Fig. 4F). CRISPR-Cas9–mediated disruption of *Hcn1* was sufficient to reduce sexual satiety after consecutive ejaculations across days without changing mating performance in male mice (Fig. 4G and fig. S18A). In whole-cell recordings, individual Cas9-expressing BNST^{Esr2} with *Hcn1* disruption showed a reduced voltage sag, increased firing threshold (rheobase), and silent spontaneous firing in a higher proportion (Fig. 4H). However, the same disruption of *Hcn1* in female BNST^{Esr2} did not restore their sexual receptiveness at 0.5 to 1 hour after mating (fig. S18B).

Discussion

The finding that BNST^{Esr2} represent sexual satiety is notable, given the lack of knowledge about where and how lasting motivational states might be encoded in the brain. Whether activated during ejaculation, soon after ejaculation (their off-dynamics remain unclear), or during sexual satiety period, BNST^{Esr2} in both sexes may commonly represent a sexual satiety state and play a particular role in reducing internal mating motivation after successful mating (Fig. 2G). A similar model (also known as the hydraulic model) was proposed by Lorenz more than 70 years ago to explain how flexible behavioral decisions are made in concert with dynamic internal motivational states (*31*). However, stimulating BNST^{Esr2} was ineffective in suppressing mating actions in virgin females but not males. How can these findings be reconciled with the common role of BNST^{Esr2} in encoding sexual satiety in both sexes? One possibility is that the activity of BNST^{Esr2} may not be sufficient to drive sexual satiety in female mice and might need other cofactors such as hormonal state. In virgin male mice, inhibition of BNST^{Esr2} also leads to indiscriminate mating behaviors, suggesting potential roles of BNST^{Esr2} in behaviors not directly related to sexual satiety.

Our findings also indicated that the post-ejaculation activation of BNST^{Esr2} in both sexes can result in long-lasting modifications of their excitability and firing threshold, which are mediated partially by HCN channels selectively in male but not female mice. This finding may be extended to the understanding of persistent changes in other forms of social behaviors as well as cognitive functions (*32*–*36*). Together, our findings revealed that experience-dependent changes in ion channels, which are effective in regulating cellular firing patterns and/or excitability, may serve as a general mechanism that contributes to long-lasting modifications in internal states.

REFERENCES AND NOTES

1. D. J. Anderson, *Nat. Rev. Neurosci.* **17**, 692–704 (2016).
2. P. Chen, W. Hong, *Neuron* **98**, 16–30 (2018).
3. D. Wei, V. Talwar, D. Lin, *Neuron* **109**, 1600–1620 (2021).
4. E. M. Hull, R. I. Wood, K. E. McKenna, in *Neurobiology of Male Sexual Behavior*, D. N. Jimmy Ed. (Academic Press, 2006), chap. 33.
5. B. V. Phillips-Farfán, A. Fernández-Guasti, *Neurosci. Biobehav. Rev.* **33**, 442–455 (2009).
6. T. E. McGill, *J. Genet. Psychol.* **103**, 53–57 (1963).
7. T. E. McGill, R. C. Coughlin, *J. Reprod. Fertil.* **21**, 215–220 (1970).
8. L. M. Coolen, H. J. Peters, J. G. Veening, *Brain Res.* **738**, 67–82 (1996).
9. M. M. Heeb, P. Yahr, *Neuroscience* **72**, 1049–1071 (1996).
10. K. K. Ishii *et al*., *Neuron* **95**, 123–137.e8 (2017).
11. T. Yamaguchi *et al*., *Nat. Neurosci.* **23**, 1111–1124 (2020).
12. C. F. Yang *et al*., *Cell* **153**, 896–909 (2013).
13. Y. C. Wei *et al*., *Nat. Commun.* **9**, 279 (2018).
14. S. Inoue *et al*., *Cell* **179**, 1393–1408.e16 (2019).
15. T. Karigo *et al*., *Nature* **589**, 258–263 (2021).
16. M. Liu, D. W. Kim, H. Zeng, D. J. Anderson, *Neuron* **110**, 841–856.e6 (2022).
17. D. W. Bayless *et al*., *Cell* **176**, 1190–1205.e20 (2019).
18. B. Yang, T. Karigo, D. J. Anderson, *Nature* **608**, 741–749 (2022).
19. S. X. Zhang *et al*., *Nature* **597**, 245–249 (2021).
20. H. W. Dong, L. W. Swanson, *J. Comp. Neurol.* **471**, 396–433 (2004).
21. Y. Li *et al*., *Cell* **171**, 1176–1190.e17 (2017).
22. R. Remedios *et al*., *Nature* **550**, 388–392 (2017).
23. J. D. Welch *et al*., *Cell* **177**, 1873–1887.e17 (2019).
24. L. Yin *et al*., *Neuron* **110**, 3000–3017.e8 (2022).
25. X. Gong *et al*., *Neuron* **107**, 38–51.e8 (2020).
26. B. P. Bean, *Nat. Rev. Neurosci.* **8**, 451–465 (2007).
27. R. B. Robinson, S. A. Siegelbaum, *Annu. Rev. Physiol.* **65**, 453–480 (2003).
28. R. Hazra *et al*., *Mol. Cell. Neurosci.* **46**, 699–709 (2011).
29. S. Jolly *et al*., *Sci. Rep.* **9**, 12353 (2019).
30. R. J. Platt *et al*., *Cell* **159**, 440–455 (2014).
31. K. Lorenz, *Symp. Soc. Exp. Biol.* **4**, 221–268 (1950).
32. S. J. Thuault *et al*., *J. Neurosci.* **33**, 13583–13599 (2013).
33. S. Stagkourakis *et al*., *Nat. Neurosci.* **21**, 834–842 (2018).
34. T. Notomi, R. Shigemoto, *J. Comp. Neurol.* **471**, 241–276 (2004).
35. D. Tsay, J. T. Dudman, S. A. Siegelbaum, *Neuron* **56**, 1076–1089 (2007).
36. M. F. Nolan *et al*., *Cell* **115**, 551–564 (2003).
37. X. Zhou *et al*., Source data of Hyperexcited limbic neurons represent sexual satiety and reduce mating motivation. Zenodo (2022); doi:10.5281/zenodo.7482944.

ACKNOWLEDGMENTS

The authors thank Q. Yang, Y. R. Yang, P. X. Wu, Y. Q. Zhang, and X. Zhao for technical help; CIBR LARC staff for animal care; the CIBR Imaging Core, Instrumentation Core, Vector Core, Genetic Manipulation Core, Oxford Instruments, and Inscopix for technical support; C. Dulac, M. M. Luo, Y. Xiang, and M. Jing for constructive comments on the manuscript; and members of the Li laboratory for helpful comments on this project. **Funding:** This work was supported by STI2030–Major Project 2021ZD0203900 (Yin.L.); Human Frontier Science Program CDA00005 (Yin.L.); The National Natural Science Foundation of China 32071012 (Yin.L.); Beijing Nova Program Z191100001119084 (Yin.L.); and China Postdoctoral Science Foundation award 2021M700454 (X.T.). **Author contributions:** Conceptualization: X.Z., A.L., X.M., and Yin.L. Methodology: X.Z., A.L., and X.M. Investigation: X.Z., A.L., X.M., Z.D., M.A., Yix.L., Y.C., W.L., X.T., and X.C. Formal analysis: X.Z., A.L., X.M., and Z.D. Funding acquisition: Yin.L., X.Z., and X.T. Supervision: Yin.L. Writing – original draft: Yin.L. Writing – review and editing: Yin.L., X.Z., A.L., and X.M. **Competing interests:** The authors declare no competing interests. **Data and materials availability:** The processed data used to generate the figures can be found at Zenodo (*37*). The custom analysis code in this paper is publicly available on GitHub (https://github.com/LiLab-CIBR/sexual-satiety).

SUPPLEMENTARY MATERIALS

science.org/doi/10.1126/science.abl4038
Materials and Methods
Supplementary Text
Figs. S1 to S18
Table S1
References (*38*–*43*)
Movie S1
MDAR Reproducibility Checklist

View/request a protocol for this paper from *Bio-protocol*.

Submitted 20 June 2022; resubmitted 28 November 2022
Accepted 27 January 2023
Published online 9 February 2023
10.1126/science.abl4038